

INTERACTIONS BETWEEN BRITTLE FRACTURE AND TWINNING IN TUNGSTEN
SUBJECTED TO COMPRESSION TESTS AT 77K

Tran-Huu-Loi*, J.P. Morniroli* and M. Gantois*

Polycrystalline and single crystals of pure tungsten were subjected to compression tests at 77 K. Brittle cracks, twins or a mixture of them were observed at the surface and inside the samples. The occurrence of these cracks and twins is analysed in order to test the three following proposals:

- cracks and twins are independently produced,
- cracks are induced by twins,
- twins are induced by cracks.

INTRODUCTION

Tungsten, like other body-centered cubic metals, undergoes a ductile-to-brittle transition temperature at which it exhibits brittle transgranular or intergranular fracture modes. This transition temperature is structure sensitive and it is usually much higher than room temperature. Therefore, it limits to a great extent the room temperature applications of tungsten.

Brittleness is favoured by low temperatures and by high deformations rates. Since these conditions are also those that favour plastic deformation by twinning, connections between brittle fracture and twinning are expected. From studies on b.c.c. metals (1, 2) and on tungsten single crystals (3-8), three possibilities have been proposed:

- twinning and brittle fracture occur independently as distinct processes,
 - brittle fractures are induced by twins,
 - twinning is induced by brittle fracture.
- But the reported results contain some inconsistencies and there is little agreement between them.

* Laboratoire de Génie Métallurgique (U.A. CNRS 159 - USG2M)
Ecole des Mines - Parc de Saurupt, 54042 NANCY-Cedex (France)

In the present study, the fracture-twinning behaviour of polycrystalline and single-crystal samples of tungsten, subjected to compression tests at 77K, is examined by means of fractographic and metallographic observations.

MECHANICAL TWINNING AND CLEAVAGE FRACTURE IN TUNGSTEN

Twinning systems in tungsten

Twinning in tungsten and in other body-centered-cubic metals occurs on {112} planes (K1 twinning planes) along a <111> direction (η_1 shear direction) with a twinning shear displacement $s = \sqrt{2}/2$.

Due to the cubic symmetry, 12 twinning systems exist. They are conveniently distinguished using the stereographic projection and the numbers 1 to 12 after Schmid and Boas (9) (Figure 1).

Figure 2, which represents one of the 12 twinning systems, indicates that the shear associated with twinning, unlike slip, only occurs in one direction along a polarized shear direction. For example, a $\sqrt{2}/2$ displacement along the $[\bar{1}11]$ direction for the $(1\bar{1}2)$ twin plane (twinning system number 8); equivalent to along $[1\bar{1}\bar{1}]$ for the $(1\bar{1}2)$ twin plane.

A shear along the reverse direction with a double displacement would produce the same effect but, in agreement with energy considerations, such a reverse shear has never been reported.

A {112} <111> twinning system will operate if two conditions are realized simultaneously:

- the resolved shear stress acting on the K1 twin plane along the shear direction η_1 is positive and high. According to Allen et al (10), Cox et al (11) and Biggs and Pratt (12), the probability of twinning increases with the shear stress.

The resolved shear stress is obtained from :

$$\tau_R = \sigma \cos \Phi \cos \lambda = \sigma s$$

- the modifications of the sample shape which result from twinning must be in accordance with the mechanical tests use to produce twinning. Due to the polarity of the twinning shear, an increase or a decrease of the sample length results from twinning. To determine these length modifications for any crystal orientation, use is made of the following relation :

$$L/L_0 = \sqrt{1 + 2s \sin \chi \cos \lambda + s^2 \sin^2 \chi}$$

Thus, if a twin system produces an increase of length ($L/L_0 > 1$) the system will only be activated in tension. Alternatively, a twin system with a resulting $L/L_0 < 1$ will be favoured in compression. Two examples are given in Figure 3 for a crystal which undergoes twinning along the $(1\bar{1}2)[\bar{1}11]$ system (system n° 8). This system

FRACTURE CONTROL OF ENGINEERING STRUCTURES – ECF 6

will be activated if a tensile stress is applied along [001] or if a compression stress acts along [100] or [010].

Table I gives for the 12 {112}<111> twinning systems the values of the Schmid factors S and the l/l₀ ratio for the 3 [001], [011] and [111] orientations which outline the stereographic unit orientation triangle. In each case, the symbol C or T indicates if the twinning system is activated in compression (C) or in tension (T).

TABLE 1 - Schmid factors and l/l₀ ratios for the 12 twinning systems.

Twin number	K1	η1	Load axis					
			[001]		[011]		[111]	
			S	l/l ₀	S	l/l ₀	S	l/l ₀
1	(112)	[111]	0.47	1.41 T			0.31	0.99 C
2	(112)	[111]	0.47	1.41 T			0.15	1.15 T
3	(211)	[111]	0.23	0.86 C	0.47	0.70 C	0.31	0.99 C
4	(211)	[111]	0.23	0.86 C	0.47	0.70 C		
5	(121)	[111]	0.23	0.86 C			0.31	0.99 C
6	(121)	[111]	0.23	0.86 C			0.15	1.15 T
7	(112)	[111]	0.47	1.41 T	0.23	1.17 T	0.15	1.15 T
8	(112)	[111]	0.47	1.41 T	0.23	1.17 T		
9	(211)	[111]	0.23	0.86 C			0.15	1.15 T
10	(211)	[111]	0.23	0.86 C			0.15	1.15 T
11	(121)	[111]	0.23	0.86 C	0.23	1.17 T	0.15	1.15 T
12	(121)	[111]	0.23	0.86 C	0.23	1.17 T	0.15	1.15 T

Twinning intersections

The 12 twinning planes can intersect each other. Five types of intersections are possible. They are <111>, <531>, <311>, <210> and <110> and have been studied by Mahajan (13). The two last types of intersections are important because they lie in the {100} potential cleavage planes. They are given in Table II. For each of these intersections, the sum of the Burgers vectors of the partial dislocations from the intersecting twins is <001>. Therefore, a large tensile stress is set up at the intersection along the cleavage plane (2).

Cleavage planes

The cleavage planes usually reported for b.c.c. metals are {100} planes but {110} cleavage planes were also reported (14).

Cleavage fracture is favoured by high tensile stresses acting on the cleavage plane. The resolved cleavage stress is obtained from:

$$\sigma_c = \sigma \cos^2 \phi$$

TABLE II - Twin intersection directions which lie in the {100} cleavage planes.

Cleavage plane	Twin systems and directions of intersection					
(100)	1-2 [021]	3-4 [011]	5-6 [012]	7-8 [021]	9-10 [011]	11-12 [012]
(010)	1-7 [201]	2-8 [201]	3-9 [102]	4-10 [102]	5-11 [101]	6-12 [101]
(001)	2-7 [110]	1-8 [110]	4-9 [120]	3-10 [120]	6-11 [210]	5-12 [210]

EXPERIMENTAL METHODS

Samples

The polycrystalline samples and the single-crystals examined in this study were prepared from as-drawn sintered rods with 4 mm diameter of non-doped tungsten. The impurity contents of the sintered tungsten are given in Table III.

TABLE III - Impurity contents of the sintered tungsten rods

Impurity in p.p.m.	Al	As	Ca	C	Cr	Fe	Mg	Mo	N	P	S	K
	20	20	10	30	20	40	10	100	20	20	20	2

Polycrystalline samples were obtained by a recrystallization treatment at 1600°C for 4 hours under high vacuum (10⁻⁴ Pa). As reported earlier, this treatment produces an equiaxed structure with an average grain size of about 0.050 mm (15).

Single-crystals with high purity were obtained by electron beam zone melting*. By using oriented seeds, [001], [011] and [111] crystals with a nearly cylindrical shape (length about 50 mm and diameter about 4 mm) were produced.

Mechanical tests

Samples were submitted to compression tests at 77K with the following deformation rates: 0.5, 1, 2 and 4 x 10⁻⁴ s⁻¹.

The compression test specimens had a cylindrical shape with a length of about 8 mm and a diameter of about 4 mm. The cylindrical

* Single crystals used in this study were elaborated in the Metallurgy Department of the School of Mines of St Etienne.

shape of the single-crystals was obtained by careful surface grinding.

Observation methods

After deformation, the lateral surfaces of the deformed samples and the fracture surfaces of the broken samples were examined using scanning electron microscopy.

Planar transverse and lateral sections were also cut in the deformed samples and electro-polished. In the case of the single crystals, the crystallographic orientations of these sections was accurately determined using the Laue and etch pits methods. These polished facets were examined mainly by optical microscopy.

EXPERIMENTAL RESULTS

After deformation at 77K, the samples contained many twins and cracks. The twins exhibit various orientations and have an average thickness of 10 μm . Usually they extend over large distances in the single crystals and terminate at the surface. Thicker twins with a lens shape and fine internal striations and twins which are indented on one side (16) are also observed.

Experimental determination of the twinning systems

A few [001] single crystals exhibit deformation at 77K without breaking so that transverse and lateral sections can be prepared and used to identify the twinning systems.

Optical micrographs of a (001) transverse section and of two lateral sections parallel to the \vec{c} axis and making a 12 degree angle with the (100) and (010) planes are given in Figure 4.

Careful examinations of the orientations of the twinning plane traces on these three sections indicate that the twinning systems encountered are the systems n° 3, 4, 5, 6, 9, 10, 11 and 12 i.e. the systems expected in compression (see Table I). Since these 8 systems have the same Schmid factor, they should occur with the same frequency. This fact is experimentally verified.

None of the twinning systems, theoretically expected in tension (systems 1, 2 and 7, 8), are observed.

Experimental determination of the crack crystallography

Large cracks parallel to the loading axis and many non-propagating small cracks also appear on the micrographs. Most of them have a direction which corresponds to the traces of the {100} planes. Sometimes, traces which at first sight do not correspond to these usual cleavage planes are observed. Careful examinations

at high magnification reveal that most of these cracks are indeed {100} cleavage planes with a step morphology (Figure 5a).

Large cracks parallel to the [001] loading axis have a resolved cleavage stress $\sigma_c = 0$. The propagation of these cracks which causes macroscopic brittle fracture is probably due to additional stresses that are established when the sample barrels (1).

Configurations of the twins and cracks

Many configurations of cracks and twins are observed in the single-crystals and in the polycrystalline samples by using metallographic and fractographic observations. The most frequent ones are:

- isolated {100} cleavage cracks,
- intersections of two {100} cleavage cracks (Figure 5 b),
- isolated twins,
- intersections of twins :
 - . when a growing twin intersects an existing twin, it can either be stopped at the intersection or it can cross the first twin. Two configurations are thus possible (figure 5 c and d) whose morphology depends on the type of intersection (13).
 - . In both cases, etch pits reveal that high stresses are located at these intersections (figure 5 e).
- internal {100} cracks extending across a twin lamella (Figure 5 f). It is reported that they may be due to hard precipitate particles which refuse to shear uniformly during twin formation (17).
- crack at a twin tip-matrix interface (Figure 6 a). A model of a twin interface consisting of partial dislocations which pile up and produce high tensile stresses can explain this crack nucleation (2).
- crack at the interface matrix/twin (Figure 6 a),
- crack between two parallel non coplanar twins (Figure 6 b),
- crack between two twin tips (Figure 6 a),
- crack between a twin and a twin tip (Figure 6 a),
- crack at the intersection of two twins. Depending on their mutual orientations, two configurations are observed :
 - . the crack extends along the twin/matrix interface of one twin lamella (Figure 6 c),
 - . the crack extends transgranularly along the {100} cleavage plane on one or two sides of the intersection (Figure 6 d and e).

We noticed that these cracks are only present at the twin intersections given in Table II.

- crack at a twin-surface intersection,
- intergranular crack at the twin/boundary intersection. They are observed in polycrystalline samples (Figure 6 f).

CONCLUSIONS

These experiments indicate that the deformation by compression of tungsten samples at 77K proceeds mainly by mechanical twinning. Only the twinning systems expected from theory really occur. The presence of many cracks is also observed. Some of them are large and lead to the macroscopic fracture of the sample. Others are small non propagating cracks which are nucleated at particular twin intersections under the action of tensile stresses created along the cleavage plane by the twinning shear displacements.

The observations of isolated twins and cracks support the proposal that twins and fracture are independently produced but many observations also indicate that some fracture nucleations are twin-induced. Nevertheless, it is difficult to attribute with certainty the macroscopic failure of the specimen to the propagation of these twin-induced cracks.

ACKNOWLEDGEMENTS

The research reported here was supported by the DRET under contract 83-520.

The authors are grateful to Dr A. Kobylanski (Department of Metallurgy of the School of Mines of St Etienne) for his interest and for the preparation of the tungsten single-crystals used in this study.

SYMBOLS USED

K1	Twinning plane
η_1	Shear direction
s	Twinning shear displacement
σ_R	Resolved shear stress (Pa)
σ	Tensile stress (Pa)
λ	Angle between the loading axis and η_1
Φ	Angle between the loading axis and the K1 normal
S	Schmid factor
OL	Segment in the crystal
l_0, l	Lengths of the segment OL before and after twinning
λ'	Angle from OL to η_1
χ	Angle from OL to K1
σ_c	Resolved cleavage stress (Pa)
ϕ	Angle between the load axis and the cleavage plane

REFERENCES

- (1) Reid, N., J. of Less-Common Metals, Vol. 9, 1965, pp. 105-122
- (2) Reid, C.N., Met. Trans. A, Vol. 12A, 1981, pp. 371-377
- (3) Schadler, H.W., Trans. of the Met. Soc. of AIME, Vol. 218, 1960, pp.640-655

- (4) Wolff, U.E., *Trans. of the Metal Soc. of AIME*, Vol. 224, 1962, pp. 327-333
- (5) Koo, R.C., *Acta Met.*, Vol. 11, 1963, pp. 1083-1095
- (6) Beardmore, P. and Hull, D., *J. of Less-Common Metals*, Vol. 9, 1965, pp. 168-180
- (7) Argon, A.S. and Maloof, S.R., *Acta Met.*, Vol. 14, 1966, pp. 1463-1468
- (8) Chupyatova, L.P., Kurdyumov, V.G., Morozova, N.P., Prokhorova, O.N. and Shishkov, V.L., *Phys. Met. Metallogr.*, Vol. 37, (1), 1974, pp. 195-197
- (9) Schmid, E. and Boas, I.W., *Plasticity of Crystals*, Hughes and Co., London, 1950, p. 72
- (10) Allen, N.P., Hopkins, B.E. and Mc Lennan, J.E., *Proc. Roy. Soc.*, Vol. A234, 1956, pp. 221-247
- (11) Cox, J.J., Horne, G.T. and Mehl, R.F., *Trans. Am. Soc. Metals*, Vol. 49, 1957, pp. 118
- (12) Biggs, W.D. and Pratt, P.L., *Acta Met.*, Vol. 6, 1958, pp. 694
- (13) Mahajan, S., *Met. Trans. A*, Vol. 12A, 1981, pp. 379-386
- (14) Cordwell, J.E. and Hull, D., *Phil. Mag.*, Vol. 26 (1), 1972, pp. 215-224
- (15) Tran-Huu-Loi, Morniroli, J.P., Gantois, M., *J. of Mat. Sc.*, Vol. 20, 1985, pp. 199-206
- (16) Sleeswyk, A.W., De Geus, A. and Helle, J.N., *Acta Met.*, Vol. 11, 1963, pp. 337-345
- (17) Reid, C.N., Gilbert, A. and Hahn, G.T., *Trans. of Met. Soc. of AIME*, Vol. 236, 1966, pp. 1024-1030

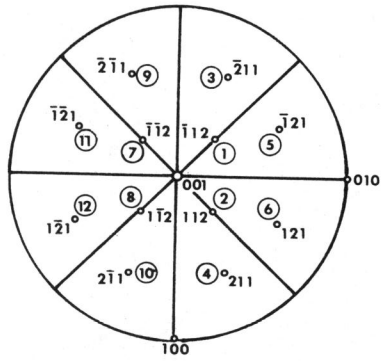


Figure 1 The 12 twinning systems after (9)

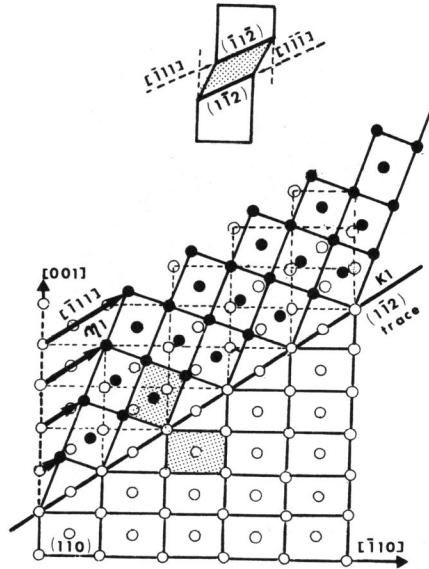


Figure 2 Representation of a twinning system

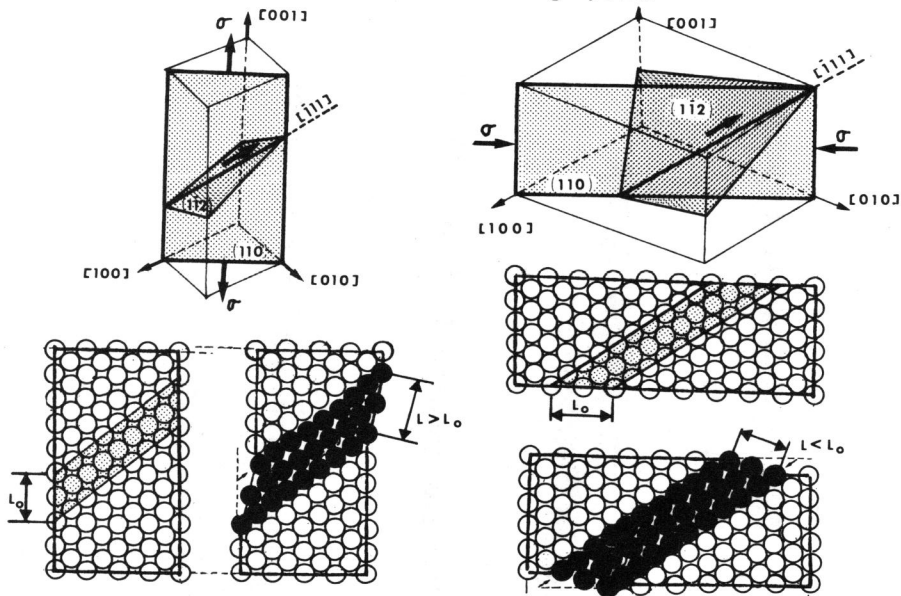


Figure 3 Variation of the length of a sample due to twinning
(a) expansion
(b) contraction

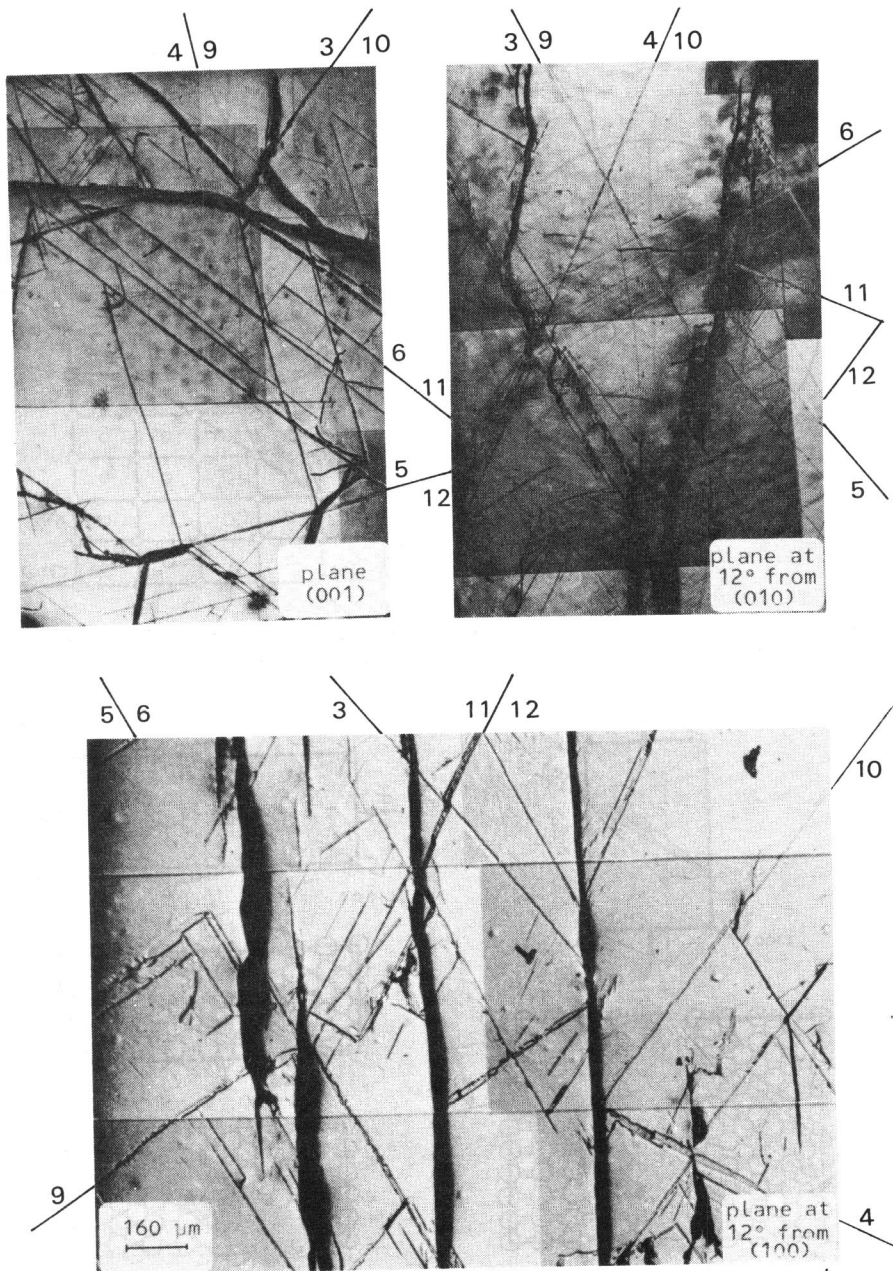


Figure 4 Transverse and lateral sections of a single crystal subjected to compression test at 77K

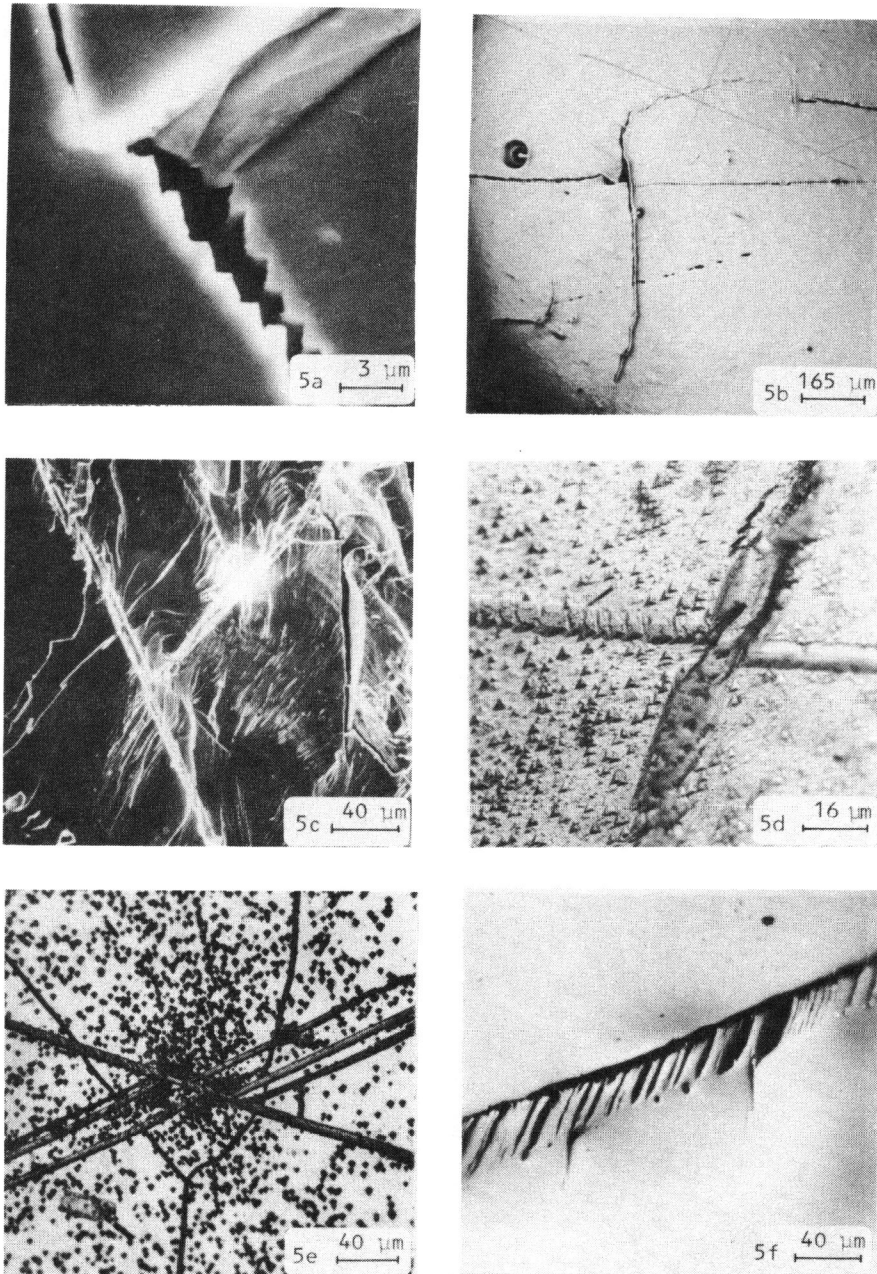


Figure 5 Various configurations of twins and cracks

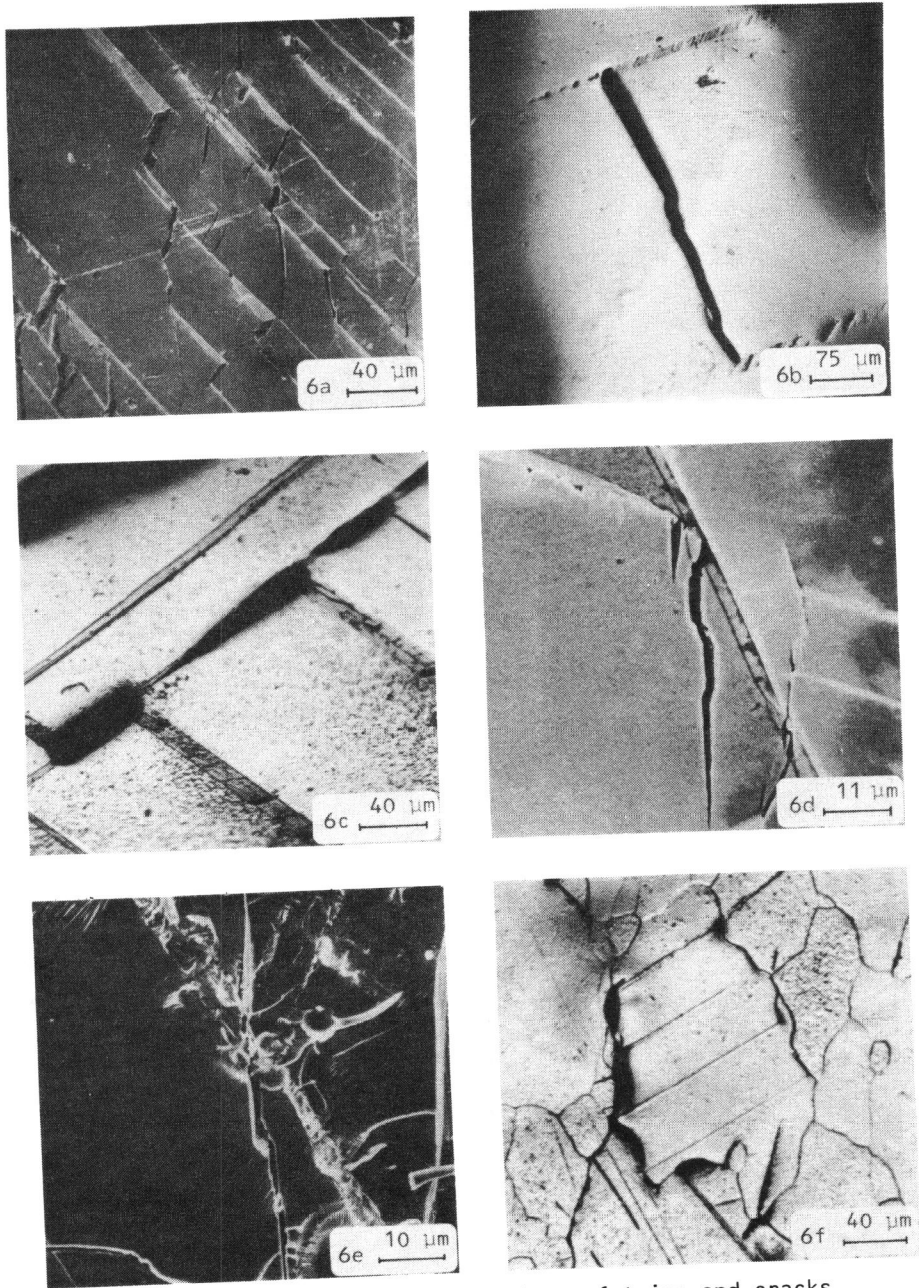


Figure 6 Various configurations of twins and cracks